Functional divergence of the Arg/N-degron pathway between the crop *Brassica rapa* and the model plant *Arabidopsis thaliana*

Brian C. Mooney[1,2], Pablo Garcia[1#], Shreenivas Singh[1#], and Emmanuelle Graciet[1*]

[1] Department of Biology, Maynooth University, Maynooth, County Kildare, Ireland

[2] Present address: Department of Biology, University of Oxford, Oxford, UK

[#] Equal author contribution

* Corresponding author: Emmanuelle.Graciet@mu.ie

Abstract

The ubiquitin-dependent Arg/N-degron pathway relates the stability of a substrate protein to the nature of its N-terminal amino acid residue or its biochemical modifications, with some N-terminal residues being recognized by specific E3 ubiquitin ligases, resulting in the ubiquitylation and degradation of the substrate protein. Work in the model plant *Arabidopsis thaliana* has shown that the Arg/N-degron pathway is a key regulator of plant responses to hypoxia, which can be either physiological or a stress in the context of waterlogging or submergence. The role of the Arg/N-degron pathway in hypoxia response is mediated *via* the oxygen-dependent degradation of group VII ETHYLENE RESPONSE FACTOR (ERF-VII) transcription factors, which act as the master regulators of the hypoxia response program in plants. Analysis of Arabidopsis mutants for different enzymatic components of the Arg/N-degron pathway has also revealed its roles in the regulation of responses to other abiotic stresses (e.g. salt stress), as well as to pathogens. Although much has been learned from studies in Arabidopsis about the functions of the Arg/N-degron pathway, very little is known about this pathway in crops, including in Brassica crops such oilseed rape, cabbage or turnip. To determine functional similarities and divergence of the Arg/N-degron pathway between Arabidopsis and Brassica crops, we isolated and characterized the first Arg/N-degron pathway mutants in *Brassica rapa* (turnip, pak choi), a diploid Brassica crop closely related to oilseed rape. We focused on two enzymatic components, namely the arginine-transferases (*ATE*s) and the E3 ubiquitin ligase *PROTEOLYSIS6* (*PRT6*). Our results show both similarities and divergence of function for these Arg/N-degron pathway components in *B. rapa* compared to Arabidopsis. Specifically, *ATE* mutants in *B. rapa* are seedling lethal, which contrasts with the mild phenotypic defects of the equivalent Arabidopsis mutants. Double mutant lines for two of the three *PRT6* genes in *B. rapa* indicated a constitutive activation of hypoxia response genes at the transcriptional level, as shown in the single mutant *prt6* in Arabidopsis. However, contrary to Arabidopsis, the *B. rapa* double mutants were more sensitive to waterlogging and hypoxia, and did not show differential response to salt stress or to biotic stress compared to the wild type. The functional divergence identified likely reflects variability in each species in the substrate repertoire and/or in the regulation of pathways or targets downstream of Arg/N-degron pathway substrates. Such differences could be driven by direct selective pressures at N-termini (e.g. gain or loss of a destabilizing

N-terminal residue), or by species-specific proteases that may generate destabilizing neo-N-termini after cleavage. These similarities and differences highlight the difficulties in translating research findings from Arabidopsis to crops, even within the same plant family (Brassicaceae) and highlight the need to study pathways in crops.

Keywords: N-degron pathway, PROTEOLYSIS 6, arginine-transferase, Brassica rapa, hypoxia, stress

Introduction

The ubiquitin/proteasome system plays essential roles in the regulation of plant responses to biotic and abiotic stresses. In plants, the ubiquitin-dependent N-degron pathway in particular functions as a key regulator of plant responses to low oxygen conditions (hypoxia) (reviewed in (Dissmeyer, 2019; Varshavsky, 2019)), which can be caused by environmental conditions such as flooding (including waterlogging or submergence) (Loreti and Perata, 2020; Weits et al., 2021). Work in the model plant *Arabidopsis thaliana* has uncovered the biochemical mechanisms underpinning the role of the N-degron pathway in mediating response to hypoxia (Gibbs et al., 2011; Licausi et al., 2011; Weits et al., 2014), but much less is known about the roles of this pathway in other plants, especially crops. The N-degron pathways relate the stability of a protein to the identity of its N-terminal residue or its post-translational modifications (reviewed in (Dissmeyer, 2019; Varshavsky, 2019)). The so-called Arg/N-degron pathway includes a number of enzymatic components that act (sequentially) to modify a substrate's N-terminal residue and bind so-called N-terminal destabilizing residues that can act as a degradation signal (degron) (Figure 1A) (Potuschak et al., 1998; Stary et al., 2003; Garzon et al., 2007; Graciet et al., 2009; Graciet et al., 2010). Several *bona fide* N-degron pathway substrates have been identified in Arabidopsis (Gibbs et al., 2011; Licausi et al., 2011; Gibbs et al., 2018; Goslin et al., 2019; Weits et al., 2019; Labandera et al., 2020), some of which are degraded in an oxygen-dependent manner, such as for example LITTLE ZIPPER 2 (ZPR2) and VERNALIZATION2 (VRN2), which regulate developmental processes in the context of physiological hypoxic niches (Gibbs et al., 2018; Weits et al., 2019; Labandera et al., 2020).

The best known substrates of the Arg/N-degron pathway are a set of five group VII ETHYLENE RESPONSE FACTOR transcription factors (collectively noted ERF-VIIs) that act as the master regulators of the transcriptional hypoxia response program (Mustroph et al., 2009; Gibbs et al., 2011; Licausi et al., 2011; Reynoso et al., 2019). Their Arg/N-degron-dependent degradation renders this pathway a key regulator of hypoxia responses and a component of the oxygen sensing mechanisms in plants. Arabidopsis *prt6* mutants, which are affected for the E3 ubiquitin ligase that ubiquitylates the ERF-VIIs, exhibit increased tolerance to waterlogging and to hypoxia due to the constitutive accumulation of the ERF-VIIs (Gibbs et al., 2011). Notably, Arabidopsis *prt6* mutants also exhibit tolerance to other

89 abiotic stresses such as high salt and drought (Vicente et al., 2017). This phenotype is
90 conserved in barley (*Hordeum vulgare*) plants expressing an RNAi construct targeting *Hv*
91 *PRT6*, suggesting that Arg/N-degron pathway components could be targets of interest to
92 improve crop tolerance to waterlogging and potentially to other abiotic stresses (Mendiondo
93 et al., 2016; Vicente et al., 2017), including osmotic stress (Papdi et al., 2015). In line with
94 this idea, the overexpression of ERF-VII homologs in crop species such as maize (Yu et al.,
95 2019) and wheat (Wei et al., 2019) results in improved tolerance to waterlogging.
96 Overexpression in Arabidopsis of the *RAP2.2* ERF-VII transcription factor also led to
97 improved resistance to the fungal necrotrophic pathogen *Botrytis cinerea*, suggesting that
98 the function of these ERF-VIIs may extend to the regulation of plant defenses against
99 pathogens (Zhao et al., 2012), perhaps due to the formation of local hypoxic niches at the
100 site of *B. cinerea* infection (Valeri et al., 2021). Similarly, overexpression in Arabidopsis of the
101 barley *RAP2.2* homolog (noted *Hv RAF*) also resulted in increased resistance to the bacterial
102 pathogen *Ralstonia solanacearum* (Jung et al., 2007). Notably, Arabidopsis mutants for Arg-
103 N-degron pathway components also showed differential defense responses to a range
104 pathogens (de Marchi et al., 2016; Gravot et al., 2016; Vicente et al., 2019). Despite this
105 knowledge and potential for applications of agronomic interest, thus far, very little is known
106 about the roles of the Arg/N-degron pathway in crops and the properties of crop plants
107 deficient for some of its components.
108 As a member of the *Brassicaceae* family, Arabidopsis is related to a range of
109 economically important crop species, including *Brassica napus* (oilseed rape), *Brassica*
110 *oleracea* (cabbage and broccoli) and *Brassica rapa* (e.g. pak choi, turnip and some oil
111 varieties). *B. rapa* may be considered as a more attractive representative model species for
112 Brassica crops because (i) its diploid genome is less complex than that of the allotetraploid *B.*
113 *napus*; (ii) the *B. rapa* Chiffu-401-42 genome was sequenced over ten years ago (Wang et al.,
114 2011); (iii) a TILLING (Targeting Induced Local Lesions In Genomes) collection of EMS
115 mutants is available (Stephenson et al., 2010); and (iv) transient expression methods are
116 available (Mooney and Graciet, 2020). Here, we sought to establish *B. rapa* as a model
117 system to investigate the functions of the Arg/N-degron pathway in Brassicaceae crops. Our
118 earlier work revealed that the enzymatic components of the Arg/N-degron pathway
119 identified in Arabidopsis are conserved in *B. rapa*, alongside additional homologs (Mooney
120 and Graciet, 2020). For example, the E3 ubiquitin ligase PROTEOLYSIS 6 (PRT6) is encoded by

121 a single gene in Arabidopsis, but by three genes in *B. rapa*. However, similarly to Arabidopsis,
122 *B. rapa* codes for two Arg-transferases. For the first time, we isolated and characterized *B.*
123 *rapa* mutants for Arg/N-degron pathway components (specifically, Arg-transferases and
124 PRT6) from the Ro18 TILLING population (Stephenson et al., 2010), and show that they have
125 both similar and divergent phenotypes to their Arabidopsis counterparts. These differences
126 could be relevant to the discovery of new functions of Arg/N-degron pathway in plants and
127 to efforts to translate findings from Arabidopsis to Brassica crops.
128

129 ## Materials and Methods

130 **Plant growth media and conditions**

131 *B. rapa* plants were grown on a sterilized soil mixture containing a 5:3:2 ratio of compost,
132 vermiculite and perlite. For experiments involving seedlings, *B. rapa* was grown in Petri-
133 dishes or sterile plastic cups containing 0.5x Murashige and Skoog (MS) medium (pH 5.7)
134 with 6 g/L agar and 0.5% (w/v) sucrose unless stated otherwise in the figure legends. Trays
135 or plates were incubated in the dark at 4°C for 3 days prior to transfer to growth rooms.
136 Plants were grown either in continuous light or in short-day conditions (8 hrs light/16hrs
137 dark), as specified below.
138

139 ***B. rapa* lines isolated**

140 *B. rapa* subsp. trilocularis (Yellow Sarson) genotype Ro18 was used. N-degron mutant lines
141 were isolated from a TILLING (Targeting Induced Local Lesions In Genomes) population
142 derived from Ro18 EMS mutagenesis (Stephenson et al., 2010) (Supplementary Table S1).
143 Seeds were obtained from RevGen UK (John Innes Centre, Norwich). The *Br ate1-2, Br*
144 *prt6.2-12* and *Br prt6.3-1* lines were backcrossed twice to the wild-type Ro18 parent and *Br*
145 *ate2-2* was backcrossed once prior to crossing to *Br ate1-2*. After crossing, F1 heterozygous
146 plants for both genes were allowed to self-fertilize in order to obtain segregating populations
147 that could be used to screen for mutant combinations.
148

149 **Genotyping of N-degron mutant *B. rapa* lines**

150 Genomic DNA was extracted as in (Edwards et al., 1991). The *Br ate1-2, Br ate2-2* and *Br*
151 *prt6.3-1* single nucleotide polymorphisms (SNPs) were genotyped using Sanger sequencing

152 following amplification of the relevant genomic region by PCR using oligonucleotides
153 BM28/BM29, BM30/BM31 and BM36/BM37, respectively (see Supplementary Table S2 for
154 oligonucleotide sequences). A dCAPS assay was used to identify the *Br prt6.2-12* SNP: a
155 nested PCR was carried out using the BM93/BM94 oligonucleotides for the external PCR and
156 BM97/BM98 for the internal PCR, followed by digestion with *Bcl*I for 6 hrs at 55°C (wild type:
157 219 bp; *Br prt6.2-12*: 199 bp and 20 bp). Presence of the mutation was confirmed by Sanger
158 sequencing after PCR with BM34/BM35.
159
160 **Reverse transcription quantitative PCR (RT-qPCR)**
161 Total RNA was extracted using the Spectrum Plant Total RNA Kit (Merck). Reverse
162 transcription reactions were set up using 100-1000 ng of isolated total RNA using RevertAid
163 Reverse Transcriptase (Thermo Fisher), RiboLock RNase inhibitor (Thermo Fisher) and
164 oligo(dT)18. qPCR reaction mixtures were set up in 96-well plates (Roche) with 1 µL of cDNA
165 mixed with 1 µL of a primer pair mixture (1 µM final concentration each) and 5 µL 2X SYBR
166 green master mix (Roche), with nuclease-free water added to a final volume of 10 µL *per*
167 well. qPCR reactions were carried out in a LightCycler 480 instrument (Roche). The second
168 derivative maximum method was used to determine crossing point (Cp) values. Gene
169 expression was calculated relative to a reference gene with the comparative Ct method
170 ($Cp_{reference\ gene} - Cp_{gene\ of\ interest}$ = deltaCp). Assuming a PCR efficiency value of 2, relative
171 expression was calculated as $2^{deltaCp}$. *Br GAPDH* (*GLYCERALDEHYDE 3-PHOSPHATE*
172 *DEHYDROGENASE;* Bra016729) was used as a reference gene for RT-qPCRs in *B. rapa* (Procko
173 et al., 2014). Oligonucleotides used for qPCR are listed in Supplementary Table S2.
174
175 **Agroinfiltration and transient expression in *B. rapa***
176 This procedure was carried out as described in (Mooney and Graciet, 2020). *A. tumefaciens*
177 C58 pGV2260 (McBride and Summerfelt, 1990) transformed with the indicated N-degron
178 pathway reporters (Graciet et al., 2010) or a pML-BART empty vector were grown for 3-4
179 days at 28°C on LB agar supplemented with 50 mg/L rifampicin, 100 mg/L ampicillin and 100
180 mg/L spectinomycin. After 3-4 days growth, bacteria were suspended from plates in 2 mL
181 infiltration medium (10 mM MES pH5.5, 10 mM $MgCl_2$, 150 µM acetosyringone) and diluted
182 to OD_{600} of 0.75. Four to five week-old *B. rapa* plants were covered with plastic lids overnight
183 prior to infiltration. A ~2 cm diameter area was marked on the abaxial side of the first and

184 second true leaves. Using a blunt 1 mL syringe, the bacterial suspension was infiltrated into
185 the marked areas. Excess liquid was removed with tissue paper and plants were returned to
186 the growth room. Tissue was harvested 3 days post agroinfiltration for protein or RNA
187 extraction.
188
189 **LUC and GUS activity assays with N-degron pathway reporter constructs**
190 All N-degron pathway reporter constructs used in this study have been previously published
191 in (Worley et al., 1998; Graciet et al., 2010). The same protocol as in (Mooney and Graciet,
192 2020) was used. Briefly, proteins were extracted from frozen ground tissue using 1X
193 Luciferase Cell Culture Lysis Reagent (Promega), supplemented with 1 mM
194 phenylmethylsulfonyl fluoride (PMSF) and 1:100 plant Protease Inhibitor Cocktail (Merck).
195 Samples were centrifuged at 12,000 x g for 10 minutes at 4°C to pellet cellular debris.
196 Protein concentration was determined using the Bradford protein assay.
197 LUC activity was measured as in (Luehrsen et al., 1992; Graciet et al., 2010; Mooney
198 and Graciet, 2020). Briefly, CCLR protein extract (1-2 µL) was added to 100 µL LAR buffer (20
199 mM tricine, pH7.8, 1.07 mM $(MgCO_3)_4$, $Mg(OH)_2.5H_2O$, 2.67 mM $MgSO_4$, 0.1 mM
200 ethylenediaminetetraacetic acid (EDTA), 33.3 mM dithiothreitol (DTT), 270 µM coenzyme A,
201 470 µM luciferin, 530 µM ATP) in a 96-well plate (Sterilin). Luminescence was measured
202 using a POLARstar Omega microplate reader (BMG LABTECH) for 10 seconds. Luminescence
203 values were then normalized to the relative expression of the *LUC* gene as determined by RT-
204 qPCR from the same tissue (see Supplementary Table S2 for oligonucleotide sequences).
205
206 ***B. rapa* flg22 treatment for RNA-Seq**
207 *B. rapa* seedlings were grown in continuous light conditions at 20°C in cups containing 0.5x
208 MS agar supplemented with 0.5% (w/v) sucrose. After 3 days, 4 seedlings *per* genotype *per*
209 treatment were transferred to a well of a 6-well plate containing 6 mL of 0.5x MS
210 supplemented with 0.5% sucrose (liquid medium) and returned to the growth room for
211 incubation overnight with mild shaking. On day 4, seedlings were treated with 1 µM flg22 or
212 an equivalent volume of water (mock treatment) for 1 hr. Seedlings were collected and
213 frozen immediately in liquid nitrogen prior to RNA extraction with Spectrum Plant Total RNA
214 Kit (Merck). Samples from three biological replicates were used.
215

216 **RNA-Seq, data processing and functional analysis**

217 RNA integrity was assessed using an Agilent 2100 Bioanalyzer (Agilent). All RNA samples had
218 RNA integrity (RIN) values >7.0. Library preparation and paired-end 100 bp next-generation
219 sequencing was performed by BGI (Hong Kong) using the DNB-seq platform. Data processing
220 was carried out by BGI using the filtering software SOAPnuke (including removal of reads
221 containing the adaptor; removal of reads whose N content is greater than 5%; and removal
222 of low-quality reads). The Hierarchical Indexing for Spliced Alignment of Transcripts (HISAT2)
223 software was then used for mapping clean reads to the *B. rapa* reference genome available
224 at the time of the study (GCF_000309985.2). Differential gene expression was determined
225 using DESeq2. Cut-offs of adjusted p-value < 0.001 and $|\log_2$ of fold-change$|$ > 1 were
226 applied to determine differentially expressed genes (DEGs). Significant enrichment analysis
227 of GO function on DEGs was carried out using ShinyGO 0.82 (Ge et al., 2020) using the
228 STRING.51351 database as reference (STRING v11.5). Overlap between datasets was
229 determined using InteractiVenn (Heberle et al., 2015), and statistical significance of the
230 overlap between datasets was calculated using 2x2 contingency tables and Chi-square tests.
231 Raw and processed data are submitted to NCBI Gene Expression Omnibus under accession
232 number GSE311966 (to be released upon manuscript publication).

233

234 **Waterlogging stress experiments**

235 Seeds were sown on sterilized soil, and pots were placed in a tray covered with a transparent
236 lid. After 3 days at 4°C, the trays were transferred to the greenhouse (16 hrs light/8hrs dark).
237 After one week of growth, the lids were removed and the plants were grown for 3 weeks, at
238 which point waterlogging treatment was applied by keeping water approximately 1 cm
239 above the soil level. After two weeks of waterlogging, SPAD measurements were taken on 2
240 different locations (each side of the midvein) of leaf 3 using a Multispeq device (PhotosynQ).

241

242 **Hypoxia treatment and chlorophyll content determination**

243 Seeds were surface-sterilised using the vapor-phase sterilization method (Lindsey et al.,
244 2017), and sown in plastic glasses with 0.5xMS agar (0.5% w/v) medium. Seeds were
245 germinated and seedlings were grown in continuous light. Seven-day-old seedlings were
246 treated with hypoxia by placing the cups into anaerojars with an anaerogen sachet (Oxoid)
247 for 16 hrs in the dark. Seedlings were then returned to continuous light conditions. After 24

248 hrs of recovery, fresh weight of the seedlings was determined and pictures were taken for
249 scoring. Chlorophyll was then extracted following the protocol described in (Sumanta et al.,
250 2014). Scores were defined as: 1 = dead seedling (completely white); 2 = seedling more than
251 40% yellow or white; 3 = seedling approximately 50% white or yellow; 4 = seedling less than
252 40% yellow or white; 5 = seedling is completely green. Five biological replicates were
253 performed with 4 seedlings/genotype, condition and replicate.
254
255 **Salt stress response assay**
256 Seeds were surface sterilized using the bleach vapor method (Lindsey et al., 2017).
257 Sterilized seeds were sown on Petri dishes with 0.8% water agar and the plates were kept for
258 24 hrs at 20°C in the dark. Seeds were then transferred to fresh 0.8% water agar plates
259 supplemented with NaCl at concentrations of 100 mM, 150 mM and 200 mM. As a control,
260 seeds were transferred to a fresh 0.8% water agar plate without NaCl. Plates were then kept
261 vertical in continuous light conditions. Seedlings were photographed at 24, 72, and 96 hrs
262 post transfer, and root lengths were measured using ImageJ (Schneider et al., 2012). For
263 each genotype and treatment, five seedlings were used, and three independent biological
264 replicates were performed.
265
266 **Inoculation with *Sclerotinia sclerotiorum***
267 A *S. sclerotiorum* sclerotium isolated from an oilseed rape field in Ireland was used to
268 propagate *S. sclerotiorum*. Subsequently, sclerotia were cultured on Potato Dextrose Agar
269 (PDA; pH 5.2 - 5.5) and incubated at 21°C for 3 days. Actively growing mycelial plugs were
270 then excised using a sterilized cork borer from the leading edge of the colony and
271 transferred to fresh PDA plates for subculturing. The plate was kept for an additional 48 hrs
272 at 21°C to obtain growing mycelia for inoculation.
273 For infection assays, fully expanded third leaves of *B. rapa* plants were used. Mycelial
274 agar plugs were excised from the colony margin and placed onto the adaxial surface of the
275 detached leaves. Inoculated leaves were then placed on 90 mm square Petri plates
276 containing 0.8% water agar to maintain humidity. Plates containing inoculated leaves were
277 incubated in short-day conditions at 21°C to facilitate infection. Necrotic lesions on the
278 leaves were photographed 24 hrs post inoculation (hpi). Lesion size was measured using the

279 ImageJ software from images acquired from five biological replicates, each containing eight
280 plants *per* treatment and *per* biological replicate.
281
282 **Measurement of apoplastic reactive oxygen species (ROS)**
283 *B. rapa* was grown 20°C for 4 weeks in short-day conditions. Discs (1 cm diameter) were
284 taken from leaves of 4-week-old plants with a cork borer. Leaf discs were then carefully
285 divided into 4 quarters with a razor blade. Each quarter-disc was placed into a separate well
286 of a white Sterilin 96-well plate (ThermoScientific) containing 200 µL dH2O with the abaxial
287 leaf surface facing upwards. The plate was then returned to the growth room for a recovery
288 period of at least 3 hrs. 100X stock solutions of luminol (Merck) (17.7 mg/mL in 200 mM
289 KOH) and horseradish peroxidase (HRP) (Fisher Scientific) (10 mg/mL in dH2O) were
290 prepared fresh. 60 µL of a luminescence solution containing 2.8 µL 100X luminol, 2.8 µL
291 100X HRP and 54.4 µL dH2O was added to each well. The plate was then transferred to a
292 POLARstar Omega microplate reader (BMG LABTECH) and luminescence was detected for 15
293 minutes to establish a baseline measurement. During this time, a 1.4 µM stock solution of
294 flg22 was prepared in dH2O. 20 µL of a 1.4 µM stock flg22 solution was added to each well,
295 bringing the total volume to 280 µL, resulting in final concentrations of 100 nM flg22, 1X
296 luminol and 1X HRP. Luminescence was detected every 120 seconds for a 60-minute period
297 after addition of flg22.
298
299 **Growth inhibition assays in the presence of flg22**
300 *B. rapa* seedlings were grown in continuous light conditions at 20°C in cups containing 0.5x
301 MS agar supplemented with 0.5% (w/v) sucrose. After 3 days, 3 seedlings per genotype per
302 treatment were transferred to a well of a 6-well plate containing 6 mL of 0.5x MS with 0.5%
303 sucrose (liquid medium) supplemented with 100 nM flg22 or an equivalent volume of
304 deionized water (mock). Seedlings were then grown in this liquid culture with mild shaking in
305 continuous light at 20°C for 7 days, at which point seedlings were weighed.
306
307 **Statistical analyses**
308 Statistics tests are presented in the figure legends for each of the relevant panels. All
309 statistical test were performed using GraphPad Prism.
310

311 ## Results

312 **Mutation of Arg-transferases in *B. rapa* causes developmental arrest**

313 One of the best studied N-degron pathway mutants in Arabidopsis is the *ate1-2 ate2-1*
314 double mutant (noted *a1a2*) which is affected for the two functionally redundant Arg-
315 transferases *AtATE1* and *AtATE2* (Graciet et al., 2009). Similarly to Arabidopsis, *B. rapa* codes
316 for two Arg-transferase homologs, *Br ATE1* and *Br ATE2*. Mutant alleles with a premature
317 stop codon were identified for both genes in a TILLING collection in the Ro18 background
318 (Stephenson et al., 2010). Specifically, the *Br ate1-2* mutation substitutes a tryptophan
319 residue at amino acid 411 with a stop codon (TGG -> TAG), while *Br ate2-2* presents a stop
320 codon (TGG -> TGA) instead of a tryptophan at amino acid 418 (Figure 1B). After
321 backcrossing each of these mutant lines with the parental Ro18 genotype to reduce the
322 impact of background mutations, *Br ate1-2*/+ and *Br ate2-2*/+ heterozygous mutant plants
323 were crossed to each other. The F2 population was screened for a *Br ate1-2 ate2-2* double
324 homozygous mutant (noted *Br a1a2*). However, no homozygous double mutants could be
325 identified after the initial screening of the F2 population. Instead, seeds from two individual
326 *Br ate1-2 ate2-2/+* (i.e. homozygous mutant for *Br ATE1* and heterozygous mutant for *Br*
327 *ATE2*) plants originating from the same segregating population were collected. The
328 segregating F3 populations obtained from these two *Br ate1-2 ate2-2*/+ parents were grown
329 on 0.5x MS plates supplemented with 0.5% sucrose. Seedlings displaying under-developed,
330 white cotyledons were consistently identified as double homozygous *Br a1a2* mutants by
331 genotyping and represented about ¼ of the populations (Figure 1C). Other seedlings in the
332 segregating population were either *Br ate1-2* or *Br ate1-2 ate2-2/+*. The *Br a1a2* seedlings
333 had shorter hypocotyls and roots compared to the Ro18 parent, *Br ate1-2* or *Br ate1-2 ate2-*
334 *2/+* seedlings (Figure 1D). Matching genotype and seed morphology further revealed that
335 seeds of the *Br a1a2* double mutants were smaller than those of genotypes which retained
336 at least one functional copy of *Br ATE2* (Figure 1C and Figure 1D), even though *Br ate1-2*
337 *ate2-2/+* seeds were also smaller than those of the Ro18 parental genotype. When left on
338 0.5x MS medium supplemented with 0.5% sucrose, *Br a1a2* seedlings did not develop
339 beyond the seedling stage. Altogether, these data indicate that, in *B. rapa*, Arg-transferases
340 play functionally redundant essential roles in early development. The seedling lethality

341 phenotype precluded further characterization of *Br a1a2* plants, both phenotypically and
342 biochemically.
343
344 **Isolation and characterization of a *B. rapa prt6.2/3* double mutant**
345 A previous BLASTp analysis identified 3 potential homologs of Arabidopsis *PRT6* in *B. rapa*
346 (noted, *Br PRT6.1*, *Br PRT6.2* and *Br PRT6.3*) (Mooney and Graciet, 2020), with *Br PRT6.2*
347 being more highly expressed in wild-type Ro18 seedlings than *Br PRT6.1* and *Br PRT6.3*
348 (Figure 2A). TILLING mutant alleles with premature stop codons for each of these *Br PRT6*
349 homologs were identified (Supplemental Table S1). To avoid an early developmental arrest
350 phenotype similar to that observed in *Br a1a2* mutants, we instead isolated a *Br prt6.2*
351 *prt6.3* double mutant (noted *Br prt6.2/3*) that retained the function of the lesser-expressed
352 *Br PRT6.1*. The *Br prt6.2-12* and *Br prt6.3-1* mutant alleles were selected because of the
353 presence of premature stop codons at amino acids 1579 (out of 1986) and 1329 (out of
354 1968), respectively. These single mutants were back-crossed into the Ro18 parental line, and
355 heterozygous individuals were then crossed to each other to isolate a *Br prt6.2/3* double
356 mutant. Two double homozygous mutant lines (noted #68 and #80) were identified in the F2
357 population. Within the same segregating F2 population, a line wild-type for both *Br PRT6.2*
358 and *Br PRT6.3* (noted WT#67) was also isolated as an additional 'wild-type' control for the
359 presence and potential effects of segregating background mutations that may have been
360 retained despite back-crossing with Ro18. Unlike *Br a1a2* double mutant plants, the *Br*
361 *prt6.2/3* double mutant lines exhibited a wild-type-like ontogeny.
362 Analysis of the expression of *Br PRT6.1*, *Br PRT6.2* and *Br PRT6.3* in the different
363 genetic backgrounds indicated that *Br PRT6.2* mRNA levels were significantly decreased in
364 the *Br prt6.2/3* double mutants, while the mRNA levels of *Br PRT6.1* and *Br PRT6.3* remained
365 similar in the double mutant or in the two wild-type backgrounds used as a control (Figure
366 2A). Critically, transient expression of Ub-X-LUC N-degron pathway reporters in leaves of
367 double mutant (*Br prt6.2/3* #68 and #80) and wild-type (Ro18 and WT#67) plants showed
368 significantly increased accumulation of Arg-LUC and Asp-LUC in each of the *Br prt6.2/3*
369 double mutant lines compared to the two wild type lines, while Met-LUC stability was the
370 same irrespective of the genetic background (Figure 2B). To further confirm the disruption of
371 N-degron pathway function in *Br prt6.2/3*, we tested whether hypoxia response genes were
372 constitutively up-regulated in *Br prt6.2/3* seedlings, as expected from constitutive

373 accumulation of *B. rapa* ERF-VII transcription factor homologs. As expected, the expression
374 of *B. rapa* hypoxia response marker genes such as *BrHB1* (Bra001958), *Br PCO2* (Bra025636)
375 and *BrHRE2* (Bra021401) was higher in average (although not always statistically significant)
376 in both *Br prt6.2/3* double mutant lines (#68 and #80) compared to the 2 wild types (Ro18
377 and #67) (Figure 2C). Altogether, PRT6 activity in *Br prt6.2/3* double mutant plants is
378 sufficiently disrupted to allow accumulation of artificial and natural N-degron pathway
379 substrates.
380
381 **Abiotic stress responses of *Br prt6.2/3* double mutant**
382 One of the most notable phenotypes of *prt6* mutant plants, both in Arabidopsis and in
383 barley, is an increased tolerance to waterlogging and to hypoxia as a result of the
384 constitutive accumulation of ERF-VII transcription factors (Gibbs et al., 2011; Mendiondo et
385 al., 2016). The tolerance to waterlogging of *Br prt6.2/3* was therefore examined. Following
386 15 days of waterlogging of 3-week-old *B. rapa* plants, SPAD measurements were taken as an
387 assessment of relative chlorophyll content. Based on these SPAD values, the waterlogging
388 treatment negatively affected all genotypes, with a stronger negative effect on the two *Br*
389 *prt6.2/3* mutant lines (Figure 3A). To complement these results, the tolerance of 7-day-old
390 seedlings to hypoxic treatment in the dark for 16 hrs was assessed following a 24-hr recovery
391 period (Figure 3B). The results suggest that the *Br prt6.2/3* double mutant lines are more
392 sensitive to hypoxia than either of the two wild-type controls. To obtain a more accurate
393 assessment of the effect of hypoxia on the seedlings, total chlorophyll levels were
394 determined (Figure 3C). Apart from *Br prt6.2/3* #80 for which no difference between
395 normoxia and hypoxia treatment was apparent, the 3 other genotypes were confirmed to be
396 negatively affected by hypoxia treatment. However, it was not possible to identify relative
397 hypoxia tolerance differences.
398 Arabidopsis *prt6* mutants have also been shown to be more tolerant to salt stress
399 (Vicente et al., 2017). Similar tests with *Br prt6.2/3* mutant lines did not detect any
400 differences between the wild-type genotypes and the double mutant lines (Figure 3D). In
401 sum, in contrast to Arabidopsis *prt6* mutant seedlings and plants, *Br prt6.2/3* exhibited
402 increased sensitivity to waterlogging and hypoxia, while salt stress did not reveal any
403 differences between the genotypes.
404

405 **Immune and biotic stress responses of *Br prt6.2/3* double mutants**

406 Arabidopsis Arg/N-degron pathway mutants have been shown to be affected for their
407 response to a range of pathogens, albeit with different resistance/susceptibility profiles (de
408 Marchi et al., 2016; Gravot et al., 2016; Vicente et al., 2019). In addition, recent findings
409 have shown connections between the transcriptional response programs to hypoxia and to
410 the model pathogen-associated molecular pattern (PAMP) flg22, which originates from the
411 bacterial flagellin protein and can be used to elicit the first branch of the plant innate
412 immune system, known as pattern-triggered immunity (PTI) (Mooney et al., 2024). To
413 investigate defense-related similarities and differences between Arabidopsis and *B. rapa*
414 Arg/N-degron pathway mutants, innate immune responses of *Br prt6.2/3* double mutants
415 were first compared to those of the two wild-type genotypes using flg22. Gene expression
416 analysis using RT-qPCR indicated that treating 3-day old seedlings with 100 µM flg22
417 treatment for 1 hr was sufficient to trigger differential expression of two PTI marker genes
418 (*Br MPK3* (Bra038281) and *Br RBOHD* (Bra020724)) in *B. rapa* (Supplemental Fig. S1A). RNA-
419 seq analysis using the same experimental conditions was performed to compare the
420 transcriptomes of the WT#67 and *Br prt6.2/3* lines. Cut-off values of adjusted p-value <
421 0.001 and $|\log_2$ of fold-change$| > 1$ were applied to determine the sets of differentially
422 expressed genes (DEGs) in flg22-treated seedlings compared to mock-treated ones (flg/m)
423 for each genotype. Similar numbers of up- (~3,900) and down-regulated (~1,700) genes were
424 identified in WT#67$^{flg/m}$ and in *Br prt6.2/3#68*$^{flg/m}$ (Figure 4A, Supplemental Dataset 1 and
425 Supplemental Dataset 2, respectively). Analysis to identify gene ontology (GO) terms that
426 were enriched in each of these two datasets retrieved expected terms, such as for example
427 'defense response' or 'response to other organism' (Figure 4B and Supplemental Dataset 1
428 and Dataset 2). Most of the top 25 GO categories identified in the WT#67$^{flg/m}$ and *Br*
429 *prt6.2/3#68*$^{flg/m}$ datasets were common to both. Categories such as 'cellular response to
430 hypoxia' and 'signal transduction' appeared in both datasets but ranked among the top 25
431 only in *Br prt6.2/3*. To further analyze differences in the transcriptional response programs
432 of WT#67 and *Br prt6.2/3#68* to flg22, we determined the overlap between the 2 datasets
433 and identified a statistically significant overlap (p-value < 10^{-4}; Chi^2 test; 4,783 common
434 DEGs) (Figure 4C). In addition, DEGs common to both datasets showed the same
435 directionality of gene expression change and a similar amplitude of up- or down-regulation
436 (Supplemental Fig. S1B).

437 Despite this large overlap, 714 and 1,059 genes were differentially regulated in only
438 one of the 2 genotypes, i.e. in the WT or in the *Br prt6.2/3* mutant, respectively. This
439 suggests some differences in the flg22 response of WT and *Br prt6.2/3* seedlings. GO analysis
440 of the 714 DEGs specific to WT#67$^{flg/m}$ revealed an enrichment for GO categories associated
441 with chloroplast function and processes (Figure 4D), including genes coding for chlorophyll
442 binding proteins, genes involved in photosynthesis or others involved in auxin and cytokinin
443 signalling. The majority of the genes in these GO categories were down-regulated in wild-
444 type seedlings in response to flg22 (Supplemental Fig. S1C). These data suggest that flg22
445 treatment of wild-type *B. rapa* seedlings triggers repression of genes involved in chloroplast
446 function and developmental processes. The 1,059 genes differentially expressed in *Br*
447 *prt6.2/3#68*$^{flg/m}$ only were, in contrast, enriched for genes linked to the movement of
448 proteins and molecules, including genes associated with the endoplasmic reticulum, vesicles
449 and transport from the plasma membrane. Genes in these GO categories coded for proteins
450 with a wide range of enzymatic and biological functions. Genes associated with the GO term
451 'Signalling' were also enriched and fell into a wide of protein functions including many E3
452 ubiquitin ligases, as well as kinases (Supplemental Dataset 2). This points to (i) a potential
453 role of Br PRT6 enzymes in the regulation of chloroplast-related processes in wild-type *B.*
454 *rapa* treated with flg22; and (ii) a potential dysfunction of protein transport in *Br prt6.2/3*
455 seedlings in response to flg22 compared to the wild type.
456 We next tested the response of the *Br prt6.2/3* mutant to flg22 in a growth inhibition
457 assays that involves 7-day co-cultivation of 3-day-old seedlings with 100 nM flg22, and found
458 that there were not statistically significant differences between the wild-type lines and the
459 mutants (Figure 4E). Similarly, apoplastic ROS production in response to flg22 treatment was
460 not different between the wild type and the *Br prt6.2/3*mutant lines (Figure 4F). Finally, we
461 assessed whether the *Br prt6.2/3* mutants exhibited a different level of resistance to the
462 necrotrophic fungus *Sclerotinia sclerotiorum*, but found no differences in lesion size area
463 between the genotypes tested (Figure 4G). In sum, the flg22 response transcriptional
464 program of *Br prt6.2/3* exhibits differences compared to that of wild-type *B. rapa* seedlings,
465 but this does not translate into defects in other PTI assays or in response to *S. sclerotiorum*.
466

467 **Discussion**

468 The Arg/N-degron pathway has been studied in detail in the model plant *Arabidopsis*
469 *thaliana*, but much less is known about the functions of its enzymatic components in crop
470 species, especially those of the Brassicaceae family such as the diploid *B. rapa*, a close
471 relative of the allotetraploid *B. napus* (oilseed rape). Here, we isolated and characterized the
472 first *B. rapa* Arg/N-degron pathway mutants from a TILLING collection (Stephenson et al.,
473 2010), focusing on two enzymatic components of the Arg/N-degron pathway, the Arg-
474 transferases ATE1/2 and the downstream E3 ubiquitin ligase PRT6 (Figure 1A). Strikingly, the
475 *Br a1a2* double mutant exhibited early developmental arrest, which is in stark contrast to
476 the mild developmental defects of Arabidopsis *ate1 ate2* double mutant plants (i.e. leaf
477 morphology defects, early outgrowth of axillary meristems, phyllotaxis defects and delayed
478 leaf senescence) (Yoshida et al., 2002; Graciet et al., 2009). The early developmental arrest
479 phenotype in *Br a1a2* points to an essential role of Arg-transferases in the regulation of
480 cellular processes at early stages of development, likely in the shoot apical meristem. In
481 Arabidopsis, the shoot meristem regulator ZPR2 is the only ZPR protein targeted for
482 degradation by the Arg/N-degron pathway in an oxygen dependent manner due to its N-
483 terminal Cys residue (Weits et al., 2019) (ZPR1/3/4 in Arabidopsis do not start with N-
484 terminal Cys). ZPR proteins interact with class III homeodomain leucine zipper (HD-ZIP III)
485 transcription factors, including REVOLUTA (REV), PHABULOSA (PHB) and PHAVOLUTA (PHV)
486 and negatively regulate their activity (Kim et al., 2008; Gruber et al., 2021). Hence plants
487 accumulating ZPR proteins, such as Arg/N-degron pathway mutants, could show similar
488 phenotypic defects as mutants with reduced HD-ZIP III transcription factor activity. BLASTp
489 analysis with Arabidopsis ZPR1/2/3/4 retrieved 11 putative ZPR protein homologs in *B. rapa*,
490 4 of which start with the Met-Cys sequence, which is characteristic of oxygen-dependent
491 substrates of the Arg/N-degron pathway (the initial Met residue is removed by methionine
492 aminopeptidases, to expose Cys at the N-terminus). This increased number of ZPR Arg/N-
493 degron substrates in *B. rapa* could result in a stronger dependency on the Arg/N-degron
494 pathway to regulate ZPR protein accumulation, which may trigger higher ZPR protein levels
495 in *Br a1a2* than in an Arabidopsis *ate1 ate2* mutant. In turn, this could result in a stronger
496 inhibition of HD-ZIP III in *B. rapa* and a more severe phenotype similar to that of Arabidopsis
497 *rev-6 phb-13* double mutant seedlings which exhibit an early arrest of development (Prigge
498 et al., 2005), a phenotype that is similar to that of *Br a1a2* double mutant plants. An
499 additional, non-mutually exclusive, possibility is that the early developmental arrest of *Br*

500 *a1a2* mutants is due to the accumulation of *B. rapa*-specific Arg-transferase substrates not
501 present in Arabidopsis and whose removal is normally required for seedling development to
502 continue. Interestingly, the developmental arrest phenotype of *Br a1a2* is reminiscent of the
503 embryonic lethality phenotype of *ate1* mice, in which the only *MmATE1* gene is knocked out
504 (Kwon et al., 2002; Brower and Varshavsky, 2009), highlighting the essential roles of Arg-
505 transferases across a broader range of eukaryotes. Our observations with *Br a1a2* also
506 illustrate the difficulties of translating results from a model plant such as Arabidopsis to
507 crops (Roeder et al., 2025; Uauy et al., 2025).
508 To by-pass the early developmental arrest phenotype of *Br a1a2*, which precluded
509 further investigation of the Arg/N-degron pathway, and to avoid working with segregating
510 populations from *Br ate1-2 ate2-2/+* parents, we isolated a *Br prt6.2/3* double mutant line
511 containing early stop codon mutations in the two (out of 3) most strongly expressed *B. rapa*
512 homologs of Arabidopsis *PRT6*. *Br prt6.2/3* mutants developed similarly to wild-type plants,
513 while showing increased stability of Asp-LUC and Arg-LUC reporters indicating that overall
514 PRT6 activity was sufficiently impaired to allow accumulation of Arg/N-degron pathway
515 substrates. This is in agreement with the constitutive up-regulation of hypoxia-response
516 genes in *Br prt6.2/3*, likely due to the stabilization of the ERF-VII transcription factors. Hence,
517 the *Br prt6.2/3* lines could be a suitable tool to study the functions of the Arg/N-degron
518 pathway in *B. rapa*.
519 Our characterization of *Br prt6.2/3* lines focused on responses to (a)biotic stresses for
520 which differences between Arabidopsis wild-type and Arg/N-degron pathway mutant have
521 been published. Arabidopsis *prt6* mutants are more tolerant to hypoxia stress (Gibbs et al.,
522 2011), as well as to submergence (Riber et al., 2015), although for the latter, contrasting
523 observation were made (Licausi et al., 2011). Here, under the experimental conditions
524 applied, *Br prt6.2/3* plants were more susceptible to waterlogging than the wild type (Figure
525 3A). Submergence and waterlogging assays yield variable results in general, with many
526 different parameters contributing to differential outcome (e.g. light/dark, humidity, etc…).
527 Here, the observed sensitivity of *Br prt6.2/3* compared to the wild type may reflect an
528 increased susceptibility of *Br prt6.2/3* roots to waterlogging stress, which may affect the
529 ability of the mutants to maintain metabolic pathways and physiological processes. However,
530 root growth survival assays are more difficult to carry out with *B. rapa* due to the larger size
531 of the seedlings/plants and the need to grow them in a vertical manner to allow the roots to

532 grown along the medium. Another possibility is that carbon metabolism and starvation
533 response in the context of waterlogging or hypoxia in *B. rapa* may be different from that of
534 Arabidopsis. However, this is unlikely to be the case, as such differences have not been
535 observed when comparing *B. napus* and Arabidopsis transcriptional responses to hypoxia, as
536 well as sugar levels (Ambros et al., 2022). We sought to test the response of the *Br prt6.2/3*
537 mutant to hypoxia. These tests also suggested that the *Br prt6.2/3* mutant is more
538 susceptible to hypoxia, even though conflicting evidence was found between the two *Br*
539 *prt6.2/3* lines used when measuring chlorophyll levels. Survival in such assays is often
540 associated with sugar metabolism and the ability to withstand starvation, however,
541 Arabidopsis and *B. napus* do not seem to show significant differences in this respect (Ambros
542 et al., 2022), and a similar situation is likely the case with *B. rapa*. In Arabidopsis, *prt6*
543 mutants have been shown to be more salt stress tolerant (Vicente et al., 2017). However, *Br*
544 *prt6.2/3* mutants behaved similarly to the wild type in our assays. One possibility is that the
545 remaining functional allele, Br PRT6.1, is sufficient to mask a phenotype.
546 In Arabidopsis, Arg/N-degron pathway mutants differ from wild type in terms of their
547 defense response to a range of pathogens (de Marchi et al., 2016; Gravot et al., 2016;
548 Vicente et al., 2019). We identified transcriptional differences in the response of the *Br*
549 *prt6.2/3* mutant to the model PAMP flg22, specifically in terms of the regulation of
550 photosynthesis-related genes (which were differentially expressed in the wild type only) and
551 of processes involved in cellular transport, signalling and protein modification (all enriched
552 amongst DEGs specific to *Br prt6.2/3*. This suggests a potential role of the Arg/N-degron
553 pathway in the regulation of PTI, despite the lack of other PTI-associated defects in the
554 double mutant. We also tested the response of the *Br prt6.2/3* mutant to the necrotrophic
555 fungal pathogen *S. sclerotinia*, but did not observe differences compared to the wild type.
556 This contrasts with the increased susceptibility of the Arabidopsis *ate1 ate2* mutant (de
557 Marchi et al., 2016), and could be the result of the remaining activity of Br PRT6.1 in the
558 double mutant.
559 In summary, the results from the Arabidopsis/*B. rapa* comparative analyses reinforce
560 the need to validate knowledge gained in model systems *via* direct experimentation in crop
561 species (Roeder et al., 2025; Uauy et al., 2025). For example, the species-specific functions
562 of the Arg/N-degron pathway identified here suggest a partial divergence of the
563 physiological roles of the Arg/N-degron pathway since the split of Arabidopsis from Brassicas

564 43 million years ago (Beilstein et al., 2010). As the Arg/N-degron pathway components and
565 structure appear to be well-conserved, this likely reflects variability in each species in the
566 substrate repertoire and/or in the regulation of pathways or targets downstream of Arg/N-
567 degron pathway substrates. Such differences could be driven by direct selective pressures at
568 N-termini (e.g. gain or loss of a destabilizing N-terminal residue), or by species-specific
569 proteases that may generate destabilizing neo-N-termini after cleavage.
570
571
572

573 **Acknowledgements**

574 This work was funded by grants 13/IA/1870 and 20/FFP-P/8433 from Science Foundation
575 Ireland (now Research Ireland) to EG. BCM was supported by an Irish Research Council PhD
576 scholarship (GOIPG/2017/2). We are grateful to Dr. Ewen Mullins (Teagasc Oak Park) for
577 supplying sclerotia of *Sclerotinia sclerotiorum*, as well as to Prof. Frank Wellmer and Dr.
578 Joseph Beegan for helpful advice regarding the analysis of RNA-seq datasets. The authors
579 confirm that they have no conflict of interest.
580

581 **Authors contributions**

582 BCM, PG, SS and EG designed the work, conducted experiments, analyzed data and wrote
583 the manuscript.
584

585 **Accession numbers:**

586 Raw and processed data are submitted to NCBI Gene Expression Omnibus under accession
587 number GSE311966 (to be released upon manuscript publication).
588

589 ## References

590 **Ambros S, Kotewitsch M, Wittig PR, Bammer B, Mustroph A** (2022) Transcriptional
591 Response of Two Brassica napus Cultivars to Short-Term Hypoxia in the Root Zone.
592 Front Plant Sci **13:** 897673
593 **Beilstein MA, Nagalingum NS, Clements MD, Manchester SR, Mathews S** (2010) Dated
594 molecular phylogenies indicate a Miocene origin for Arabidopsis thaliana. Proc Natl
595 Acad Sci U S A **107:** 18724-18728
596 **Brower CS, Varshavsky A** (2009) Ablation of arginylation in the mouse N-end rule pathway:
597 loss of fat, higher metabolic rate, damaged spermatogenesis, and neurological
598 perturbations. PLoS One **4:** e7757
599 **de Marchi R, Sorel M, Mooney B, Fudal I, Goslin K, Kwasniewska K, Ryan PT, Pfalz M,**
600 **Kroymann J, Pollmann S, Feechan A, Wellmer F, Rivas S, Graciet E** (2016) The N-end
601 rule pathway regulates pathogen responses in plants. Sci Rep **6:** 26020
602 **Dissmeyer N** (2019) Conditional Protein Function via N-Degron Pathway-Mediated
603 Proteostasis in Stress Physiology. Annu Rev Plant Biol **70:** 83-117
604 **Edwards K, Johnstone C, Thompson C** (1991) A simple and rapid method for the preparation
605 of plant genomic DNA for PCR analysis. Nucleic Acids Res **19:** 1349
606 **Garzon M, Eifler K, Faust A, Scheel H, Hofmann K, Koncz C, Yephremov A, Bachmair A**
607 (2007) PRT6/At5g02310 encodes an Arabidopsis ubiquitin ligase of the N-end rule
608 pathway with arginine specificity and is not the CER3 locus. FEBS Lett **581:** 3189-3196
609 **Ge SX, Jung D, Yao R** (2020) ShinyGO: a graphical gene-set enrichment tool for animals and
610 plants. Bioinformatics **36:** 2628-2629
611 **Gibbs DJ, Lee SC, Isa NM, Gramuglia S, Fukao T, Bassel GW, Correia CS, Corbineau F,**
612 **Theodoulou FL, Bailey-Serres J, Holdsworth MJ** (2011) Homeostatic response to
613 hypoxia is regulated by the N-end rule pathway in plants. Nature **479:** 415-418
614 **Gibbs DJ, Tedds HM, Labandera AM, Bailey M, White MD, Hartman S, Sprigg C, Mogg SL,**
615 **Osborne R, Dambire C, Boeckx T, Paling Z, Voesenek L, Flashman E, Holdsworth MJ**
616 (2018) Oxygen-dependent proteolysis regulates the stability of angiosperm polycomb
617 repressive complex 2 subunit VERNALIZATION 2. Nat Commun **9:** 5438
618 **Goslin K, Eschen-Lippold L, Naumann C, Linster E, Sorel M, Klecker M, de Marchi R, Kind A,**
619 **Wirtz M, Lee J, Dissmeyer N, Graciet E** (2019) Differential N-end Rule Degradation of
620 RIN4/NOI Fragments Generated by the AvrRpt2 Effector Protease. Plant Physiol **180:**
621 2272-2289
622 **Graciet E, Mesiti F, Wellmer F** (2010) Structure and evolutionary conservation of the plant
623 N-end rule pathway. Plant J **61:** 741-751
624 **Graciet E, Walter F, Maoileidigh DO, Pollmann S, Meyerowitz EM, Varshavsky A, Wellmer F**
625 (2009) The N-end rule pathway controls multiple functions during Arabidopsis shoot
626 and leaf development. Proc Natl Acad Sci U S A **106:** 13618-13623
627 **Gravot A, Richard G, Lime T, Lemarie S, Jubault M, Lariagon C, Lemoine J, Vicente J, Robert-**
628 **Seilaniantz A, Holdsworth MJ, Manzanares-Dauleux MJ** (2016) Hypoxia response in
629 Arabidopsis roots infected by Plasmodiophora brassicae supports the development
630 of clubroot. BMC Plant Biol **16:** 251
631 **Gruber AV, Kosty M, Jami-Alahmadi Y, Wohlschlegel JA, Long JA** (2021) The dynamics of HD-
632 ZIP III - ZPR protein interactions play essential roles in embryogenesis, meristem
633 function and organ development. bioRxiv**:** 2021.2011.2024.469949

634 **Heberle H, Meirelles GV, da Silva FR, Telles GP, Minghim R** (2015) InteractiVenn: a web-
635 based tool for the analysis of sets through Venn diagrams. BMC Bioinformatics **16:**
636 169
637 **Jung J, Won SY, Suh SC, Kim H, Wing R, Jeong Y, Hwang I, Kim M** (2007) The barley ERF-type
638 transcription factor HvRAF confers enhanced pathogen resistance and salt tolerance
639 in Arabidopsis. Planta **225:** 575-588
640 **Kim YS, Kim SG, Lee M, Lee I, Park HY, Seo PJ, Jung JH, Kwon EJ, Suh SW, Paek KH, Park CM**
641 (2008) HD-ZIP III activity is modulated by competitive inhibitors via a feedback loop in
642 Arabidopsis shoot apical meristem development. Plant Cell **20:** 920-933
643 **Kwon YT, Kashina AS, Davydov IV, Hu RG, An JY, Seo JW, Du F, Varshavsky A** (2002) An
644 essential role of N-terminal arginylation in cardiovascular development. Science **297:**
645 96-99
646 **Labandera AM, Tedds HM, Bailey M, Sprigg C, Etherington RD, Akintewe O, Kalleechurn G,**
647 **Holdsworth MJ, Gibbs DJ** (2020) The PRT6 N-degron pathway restricts
648 VERNALIZATION 2 to endogenous hypoxic niches to modulate plant development.
649 New Phytol
650 **Licausi F, Kosmacz M, Weits DA, Giuntoli B, Giorgi FM, Voesenek LA, Perata P, van Dongen**
651 **JT** (2011) Oxygen sensing in plants is mediated by an N-end rule pathway for protein
652 destabilization. Nature **479:** 419-422
653 **Lindsey BE, 3rd, Rivero L, Calhoun CS, Grotewold E, Brkljacic J** (2017) Standardized Method
654 for High-throughput Sterilization of Arabidopsis Seeds. J Vis Exp
655 **Loreti E, Perata P** (2020) The Many Facets of Hypoxia in Plants. Plants (Basel) **9**
656 **Luehrsen KR, de Wet JR, Walbot V** (1992) Transient expression analysis in plants using firefly
657 luciferase reporter gene. Meth Enzymol **216:** 397-414
658 **McBride KE, Summerfelt KR** (1990) Improved binary vectors for Agrobacterium-mediated
659 plant transformation. Plant Mol Biol **14:** 269-276
660 **Mendiondo GM, Gibbs DJ, Szurman-Zubrzycka M, Korn A, Marquez J, Szarejko I,**
661 **Maluszynski M, King J, Axcell B, Smart K, Corbineau F, Holdsworth MJ** (2016)
662 Enhanced waterlogging tolerance in barley by manipulation of expression of the N-
663 end rule pathway E3 ligase PROTEOLYSIS6. Plant Biotechnol J **14:** 40-50
664 **Mooney BC, Doorly CM, Mantz M, Garcia P, Huesgen PF, Graciet E** (2024) Hypoxia represses
665 pattern-triggered immune responses in Arabidopsis. Plant Physiol **196:** 2064-2077
666 **Mooney BC, Graciet E** (2020) A simple and efficient Agrobacterium-mediated transient
667 expression system to dissect molecular processes in Brassica rapa and Brassica
668 napus. Plant Direct **4:** e00237
669 **Mustroph A, Zanetti ME, Jang CJ, Holtan HE, Repetti PP, Galbraith DW, Girke T, Bailey-**
670 **Serres J** (2009) Profiling translatomes of discrete cell populations resolves altered
671 cellular priorities during hypoxia in Arabidopsis. Proc Natl Acad Sci U S A **106:** 18843-
672 18848
673 **Papdi C, Perez-Salamo I, Joseph MP, Giuntoli B, Bogre L, Koncz C, Szabados L** (2015) The low
674 oxygen, oxidative and osmotic stress responses synergistically act through the
675 ethylene response factor VII genes RAP2.12, RAP2.2 and RAP2.3. Plant J **82:** 772-784
676 **Potuschak T, Stary S, Schlogelhofer P, Becker F, Nejinskaia V, Bachmair A** (1998) PRT1 of
677 Arabidopsis thaliana encodes a component of the plant N-end rule pathway. Proc
678 Natl Acad Sci U S A **95:** 7904-7908

Prigge MJ, Otsuga D, Alonso JM, Ecker JR, Drews GN, Clark SE (2005) Class III homeodomain-leucine zipper gene family members have overlapping, antagonistic, and distinct roles in Arabidopsis development. Plant Cell **17:** 61-76

Procko C, Crenshaw CM, Ljung K, Noel JP, Chory J (2014) Cotyledon-Generated Auxin Is Required for Shade-Induced Hypocotyl Growth in Brassica rapa. Plant Physiol **165:** 1285-1301

Reynoso MA, Kajala K, Bajic M, West DA, Pauluzzi G, Yao AI, Hatch K, Zumstein K, Woodhouse M, Rodriguez-Medina J, Sinha N, Brady SM, Deal RB, Bailey-Serres J (2019) Evolutionary flexibility in flooding response circuitry in angiosperms. Science **365:** 1291-1295

Riber W, Muller JT, Visser EJ, Sasidharan R, Voesenek LA, Mustroph A (2015) The greening after extended darkness1 is an N-end rule pathway mutant with high tolerance to submergence and starvation. Plant Physiol **167:** 1616-1629

Roeder AHK, Bent A, Lovell JT, McKay JK, Bravo A, Medina-Jimenez K, Morimoto KW, Brady SM, Hua L, Hibberd JM, Zhong S, Cardinale F, Visentin I, Lovisolo C, Hannah MA, Webb AAR (2025) Lost in translation: What we have learned from attributes that do not translate from Arabidopsis to other plants. Plant Cell **37**

Schneider CA, Rasband WS, Eliceiri KW (2012) NIH Image to ImageJ: 25 years of image analysis. Nat Methods **9:** 671-675

Stary S, Yin XJ, Potuschak T, Schlogelhofer P, Nizhynska V, Bachmair A (2003) PRT1 of Arabidopsis is a ubiquitin protein ligase of the plant N-end rule pathway with specificity for aromatic amino-terminal residues. Plant Physiol **133:** 1360-1366

Stephenson P, Baker D, Girin T, Perez A, Amoah S, King GJ, Ostergaard L (2010) A rich TILLING resource for studying gene function in Brassica rapa. BMC Plant Biol **10:** 62

Sumanta N, Haque CI, Nishika J, Suprakash R (2014) Spectrophotometric Analysis of Chlorophylls and Carotenoids from Commonly Grown Fern Species by Using Various Extracting Solvents. Research Journal of Chemical Sciences **4:** 63-69

Uauy C, Nelissen H, Chan RL, Napier JA, Seung D, Liu L, McKim SM (2025) Challenges of translating Arabidopsis insights into crops. Plant Cell **37**

Valeri MC, Novi G, Weits DA, Mensuali A, Perata P, Loreti E (2021) Botrytis cinerea induces local hypoxia in Arabidopsis leaves. New Phytol **229:** 173-185

Varshavsky A (2019) N-degron and C-degron pathways of protein degradation. Proc Natl Acad Sci U S A **116:** 358-366

Vicente J, Mendiondo GM, Movahedi M, Peirats-Llobet M, Juan YT, Shen YY, Dambire C, Smart K, Rodriguez PL, Charng YY, Gray JE, Holdsworth MJ (2017) The Cys-Arg/N-End Rule Pathway Is a General Sensor of Abiotic Stress in Flowering Plants. Curr Biol **27:** 3183-3190 e3184

Vicente J, Mendiondo GM, Pauwels J, Pastor V, Izquierdo Y, Naumann C, Movahedi M, Rooney D, Gibbs DJ, Smart K, Bachmair A, Gray JE, Dissmeyer N, Castresana C, Ray RV, Gevaert K, Holdsworth MJ (2019) Distinct branches of the N-end rule pathway modulate the plant immune response. New Phytol **221:** 988-1000

**Wang X, Wang H, Wang J, Sun R, Wu J, Liu S, Bai Y, Mun JH, Bancroft I, Cheng F, Huang S, Li X, Hua W, Wang J, Wang X, Freeling M, Pires JC, Paterson AH, Chalhoub B, Wang B, Hayward A, Sharpe AG, Park BS, Weisshaar B, Liu B, Li B, Liu B, Tong C, Song C, Duran C, Peng C, Geng C, Koh C, Lin C, Edwards D, Mu D, Shen D, Soumpourou E, Li F, Fraser F, Conant G, Lassalle G, King GJ, Bonnema G, Tang H, Wang H, Belcram H, Zhou H, Hirakawa H, Abe H, Guo H, Wang H, Jin H, Parkin IA, Batley J, Kim JS, Just J,

Li J, Xu J, Deng J, Kim JA, Li J, Yu J, Meng J, Wang J, Min J, Poulain J, Wang J, Hatakeyama K, Wu K, Wang L, Fang L, Trick M, Links MG, Zhao M, Jin M, Ramchiary N, Drou N, Berkman PJ, Cai Q, Huang Q, Li R, Tabata S, Cheng S, Zhang S, Zhang S, Huang S, Sato S, Sun S, Kwon SJ, Choi SR, Lee TH, Fan W, Zhao X, Tan X, Xu X, Wang Y, Qiu Y, Yin Y, Li Y, Du Y, Liao Y, Lim Y, Narusaka Y, Wang Y, Wang Z, Li Z, Wang Z, Xiong Z, Zhang Z (2011) The genome of the mesopolyploid crop species Brassica rapa. Nat Genet **43:** 1035-1039

Wei X, Xu H, Rong W, Ye X, Zhang Z (2019) Constitutive expression of a stabilized transcription factor group VII ethylene response factor enhances waterlogging tolerance in wheat without penalizing grain yield. Plant Cell Environ **42:** 1471-1485

Weits DA, Giuntoli B, Kosmacz M, Parlanti S, Hubberten HM, Riegler H, Hoefgen R, Perata P, van Dongen JT, Licausi F (2014) Plant cysteine oxidases control the oxygen-dependent branch of the N-end-rule pathway. Nat Commun **5:** 3425

Weits DA, Kunkowska AB, Kamps NCW, Portz KMS, Packbier NK, Nemec Venza Z, Gaillochet C, Lohmann JU, Pedersen O, van Dongen JT, Licausi F (2019) An apical hypoxic niche sets the pace of shoot meristem activity. Nature **569:** 714-717

Weits DA, van Dongen JT, Licausi F (2021) Molecular oxygen as a signaling component in plant development. New Phytol **229:** 24-35

White MD, Klecker M, Hopkinson RJ, Weits DA, Mueller C, Naumann C, O'Neill R, Wickens J, Yang J, Brooks-Bartlett JC, Garman EF, Grossmann TN, Dissmeyer N, Flashman E (2017) Plant cysteine oxidases are dioxygenases that directly enable arginyl transferase-catalysed arginylation of N-end rule targets. Nat Commun **8:** 14690

Worley CK, Ling R, Callis J (1998) Engineering in vivo instability of firefly luciferase and Escherichia coli beta-glucuronidase in higher plants using recognition elements from the ubiquitin pathway. Plant Mol Biol **37:** 337-347

Yoshida S, Ito M, Callis J, Nishida I, Watanabe A (2002) A delayed leaf senescence mutant is defective in arginyl-tRNA:protein arginyltransferase, a component of the N-end rule pathway in Arabidopsis. Plant J **32:** 129-137

Yu F, Liang K, Fang T, Zhao H, Han X, Cai M, Qiu F (2019) A group VII ethylene response factor gene, ZmEREB180, coordinates waterlogging tolerance in maize seedlings. Plant Biotechnol J **17:** 2286-2298

Zhao Y, Wei T, Yin KQ, Chen Z, Gu H, Qu LJ, Qin G (2012) Arabidopsis RAP2.2 plays an important role in plant resistance to Botrytis cinerea and ethylene responses. New Phytol **195:** 450-460

762 **Figures**

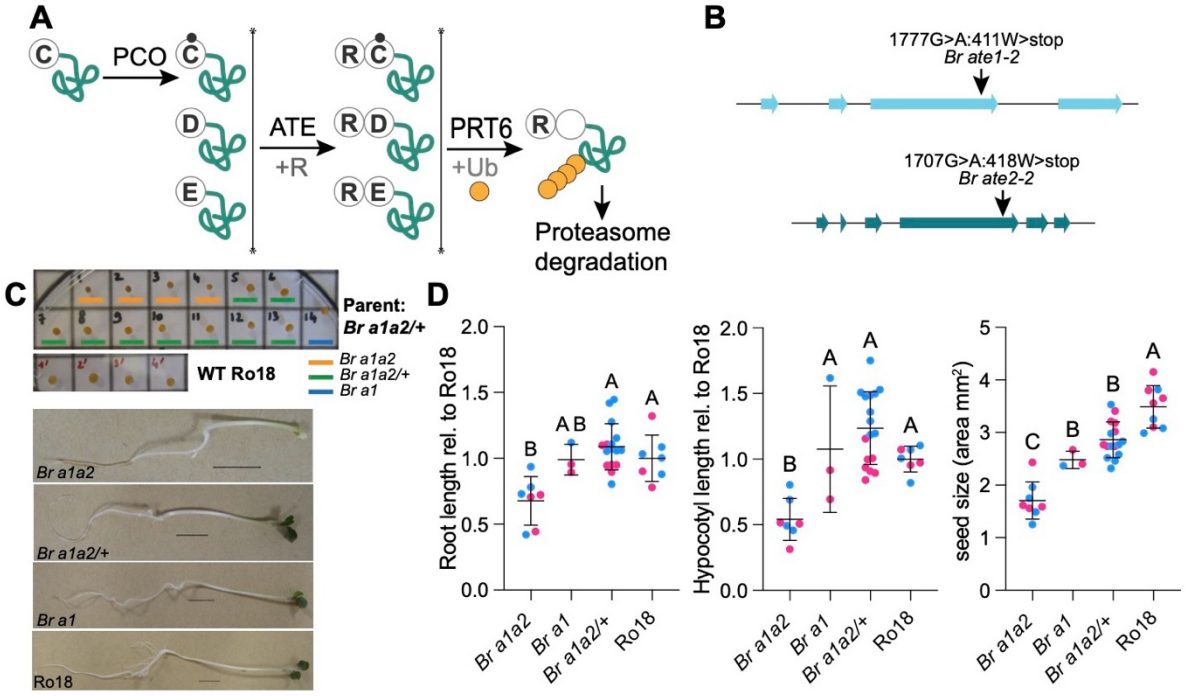

763

764 **Figure 1: Phenotype of a *Br a1a2* mutant. (A)** Overview of the Arg/N-degron pathway and
765 its enzymatic components. PLANT CYSTEINE OXIDASE (PCO) are oxygen-dependent enzymes
766 that oxidize the N-terminal Cys (C) residue of proteins (Weits et al., 2014; White et al., 2017).
767 Their substrates can then be arginylated by ATE enzymes, which also conjugate Arg (R) to
768 substrates with N-terminal Asp (D) and Glu (E) (Graciet et al., 2009; Graciet et al., 2010).
769 Arginylation is followed by recognition and ubiquitylation mediated by the E3 ubiquitin
770 ligase PROTEOLYSIS 6 (PRT6), and degradation by the proteasome (Garzon et al., 2007). PRT6
771 also recognizes proteins that start with other positively charged residues such as lysine (not
772 depicted) (Garzon et al., 2007). **(B)** Gene structure of *Br ATE1* and *Br ATE2* and position of
773 the point mutations in *Br ate1-2* (*Br a1*) and *Br ate2-2* (*Br a2*). Base pair numbering starts at
774 the ATG of the genomic locus. Amino acid substitutions and their position in the protein are
775 indicated. W: tryptophan. **(C)** Seed and seedling phenotype in the offspring population of a
776 *Br a1a2*/+ parent compared to the Ro18 wild type. *Br a1a2*: double homozygous mutant; *Br*
777 *a1a2/+:* homozygous mutant for *Br ATE1* and heterozygous mutant for *Br ATE2*; *Br a1*: single
778 homozygous mutant for *Br ATE1*. Seedlings were grown under continuous light (20°C) on
779 0.5xMS agar medium supplemented with 1% (w/v) sucrose. Pictures were taken after 4 days
780 of growth. Scale bar = 1 cm. **(D)** Quantitation of the phenotypes shown in (C), including seed
781 size area, root length relative to that of the average Ro18, hypocotyl length relative to the

average Ro18. Mean and standard deviations are shown. Statistical analysis: ANOVA and Tukey *post hoc* test; significant differences: p-value < 0.05. Pink symbols: data obtained from offspring of parent #5 (*Br a1a2*/+); blue symbols: data from offspring of parent #8 (*Br a1a2*/+). Each symbol represents individual seeds/seedlings from a given biological replicate. Data from 2 biological replicates.

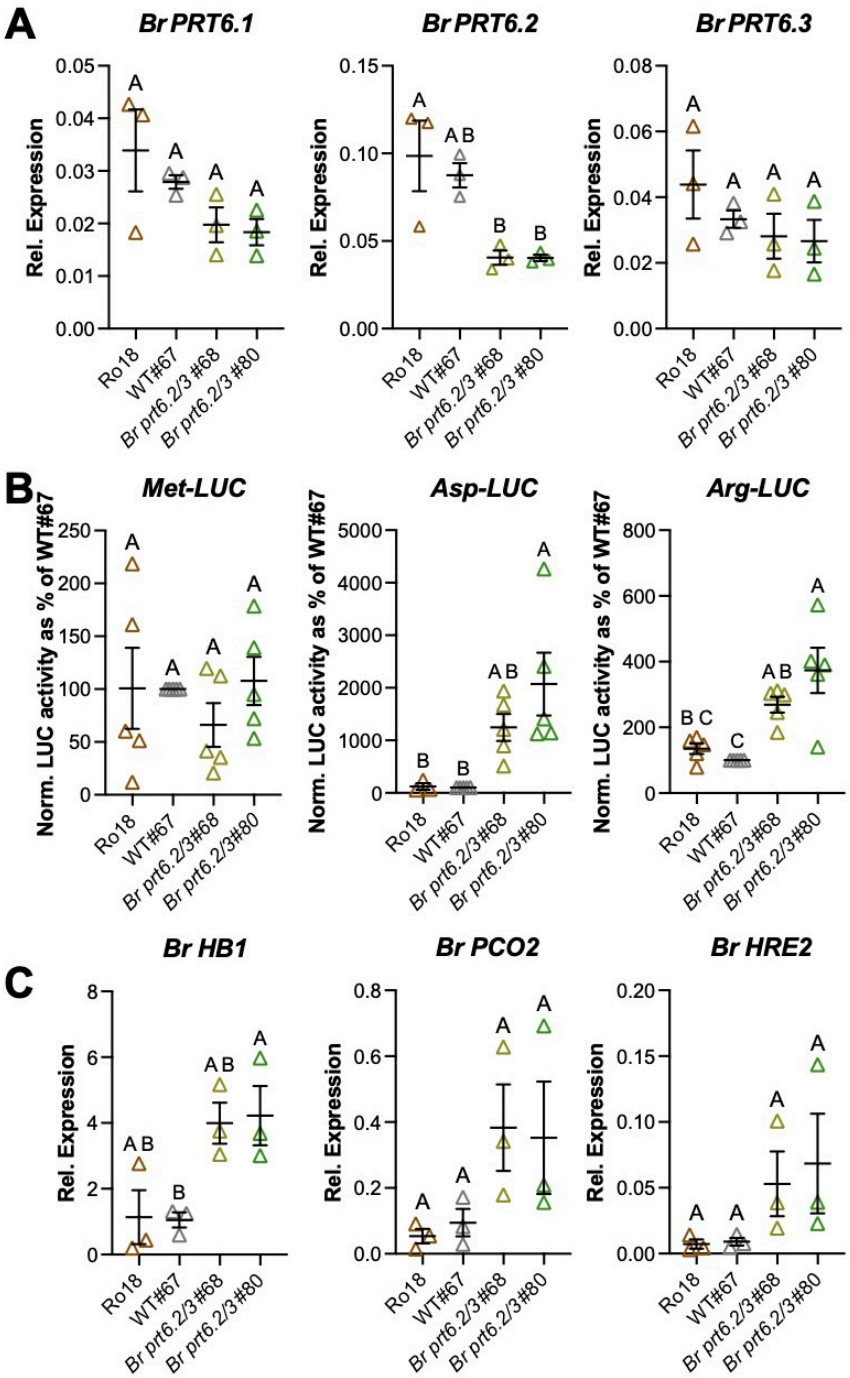

Figure 2: Accumulation of Br PRT6 substrates in *Br prt6.2/3* double mutant lines. (A) Expression of *Br PRT6.1*, *Br PRT6.2* and *Br PRT6.3* in 3-day-old seedlings of the wild type and *Br prt6.2/3* mutant. Expression was determined using RT-qPCR. The individual relative expression values to the reference gene (*Br GAPDH*) for 3 biological replicates are shown, together with the mean and standard error of the mean (SEM). Statistical significance (p-value < 0.05) is presented using the CLD format following one-way ANOVA and Tukey's test. **(B)** N-degron pathway reporter constructs stability in wild type and *Br prt6.2/3* double

795 mutant lines in transient expression assays. LUC activities normalized for LUC transcript
796 levels were determined and are presented as a percentage of the activity in the WT#67 line.
797 Data represent mean and SEM of 5 biological replicates. Statistical significance (p-value <
798 0.05) is presented using the CLD format following one-way ANOVA and Tukey's test. **(C)**
799 Expression of hypoxia response marker genes in 3-day-old wild type and *Br prt6.2/3*
800 seedlings grown on 0.5xMS supplemented with 0.5% sucrose plates. Relative expression
801 levels to the *BrGAPDH* reference gene was determined using RT-qPCR. Mean and SEM of 3
802 biological replicates are shown. Statistical significance (p-value < 0.05) is presented using the
803 CLD format following one-way ANOVA and Tukey's test.

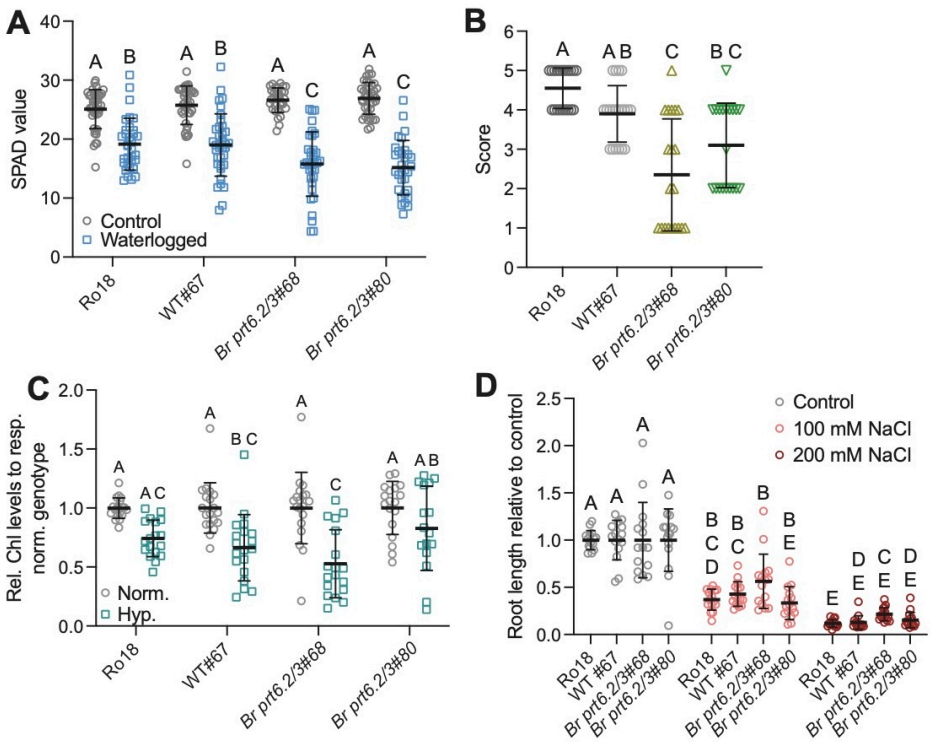

Figure 3: Response of the *Br prt6.2/3* mutant to abiotic stresses. (A) SPAD values obtained after a 14-day waterlogging treatment or of control plants kept under normal watering conditions. Mean with standard deviations (SD) of 4 biological reps (8 plants *per* treatment *per* biological replicate) are shown. Statistical significance was assessed by two-way ANOVA with Sidak's multiple comparison test. **(B)** Score of seedling health following hypoxia treatment for 16 hrs in the dark, followed by a 24-hr recovery period. Mean scores with SD of 5 biological replicates are shown (4 seedlings/biological replicate). Statistical significance was assessed using one-way ANOVA, followed by Tukey's test. **(C)** Total chlorophyll (chl) (chla+chlb) levels relative to those in the same genotype left under normoxic conditions. Mean and SD are shown from 5 biological replicates with 4 seedlings/biological replicate (except replicate 1, which had only 2 seedlings). Two-way ANOVA with Sidak's multiple comparison test was used to assess statistical significance of differences. **(D)** Root length (in cm) of seedlings grown for 72 hrs with 100 mM or 200 mM NaCl, or mock-treated. For each genotype and treatment, five seedlings were used, and three biological replicates were performed. Two-way ANOVA with Tukey's multiple comparison test was used to assess statistical significance of differences.

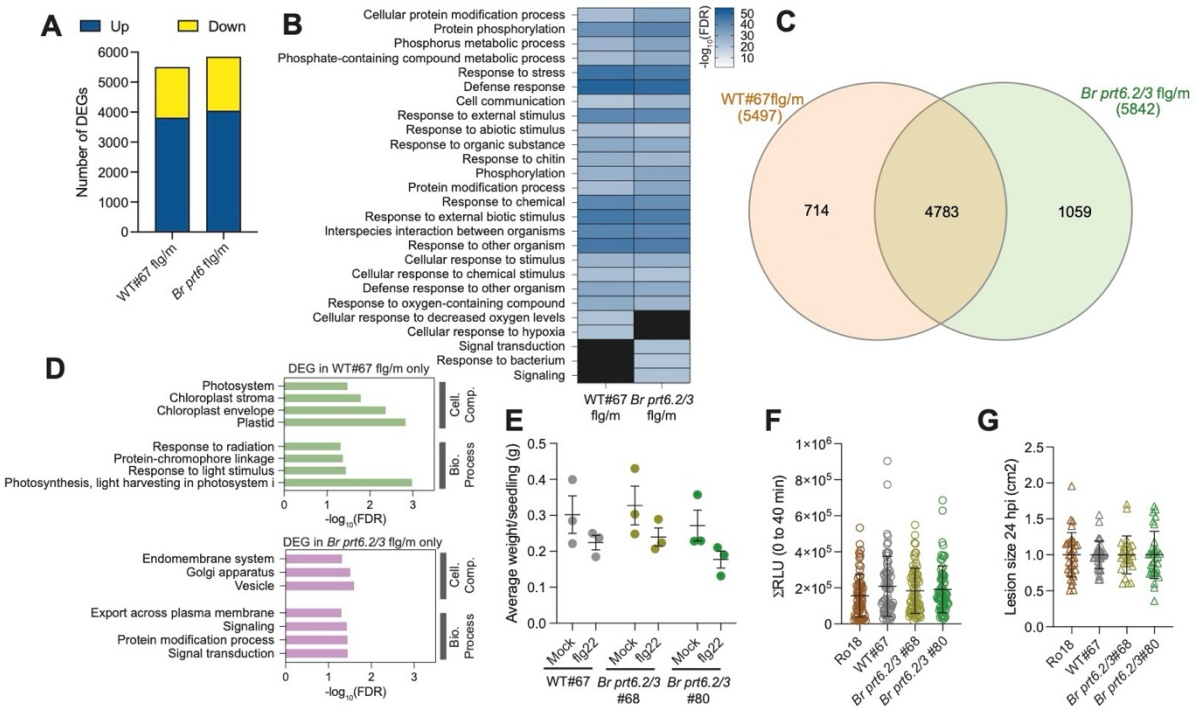

Figure 4: Response of *Br prt6.2/3* mutants to flg22 and *S. sclerotiorum*. (A) Number of DEGs in WT#67 and in *Br prt6.2/3*#68 (*Br prt6*) when comparing flg22-treated to mock-treated seedlings (flg/mock) with adj. p <0.001 and |log2FC| > 1.0. **(B)** Top 25 GO Biological Process terms obtained using ShinyGO v0.82 (FDR < 0.05). Most of the GO terms are common to the two datasets, except for 5 GO terms which are unique to either one of the two datasets. **(C)** Overlap and differences between the WT#67$^{flg/m}$ and in *Br prt6.2/3*#68$^{flg/m}$ DEGs. **(D)** GO analysis to determine enrichment for 'Biological Process' and also for 'Cellular Compartment' amongst the 714 DEGs specific to WT#67$^{flg/m}$ (green) and the 1,059 DEGs in *Br prt6.2/3*#68$^{flg/m}$ (pink) only (FDR < 0.05). **(E)** Growth inhibition with 3-day old seedlings co-cultivated with 100 nM flg22 for 7 days. Mean and SEM from 3 biological replicates are shown. No statistically significant differences after 2-way ANOVA. **(F)** ROS production assay. Datapoints represent means of 72 readings (leaf-disc quarters) taken from 18 leaf discs over 3 independent replicates. Error bars indicate SEM. RLU = Relative Light Units. No statistically significant differences after one-way ANOVA. **(G)** Lesion area measured 24 hpi with *S. sclerotiorum*. Mean and SD of 5 biological replicates are shown with 3-8 plants per replicate. No statistically significant differences after one-way ANOVA.

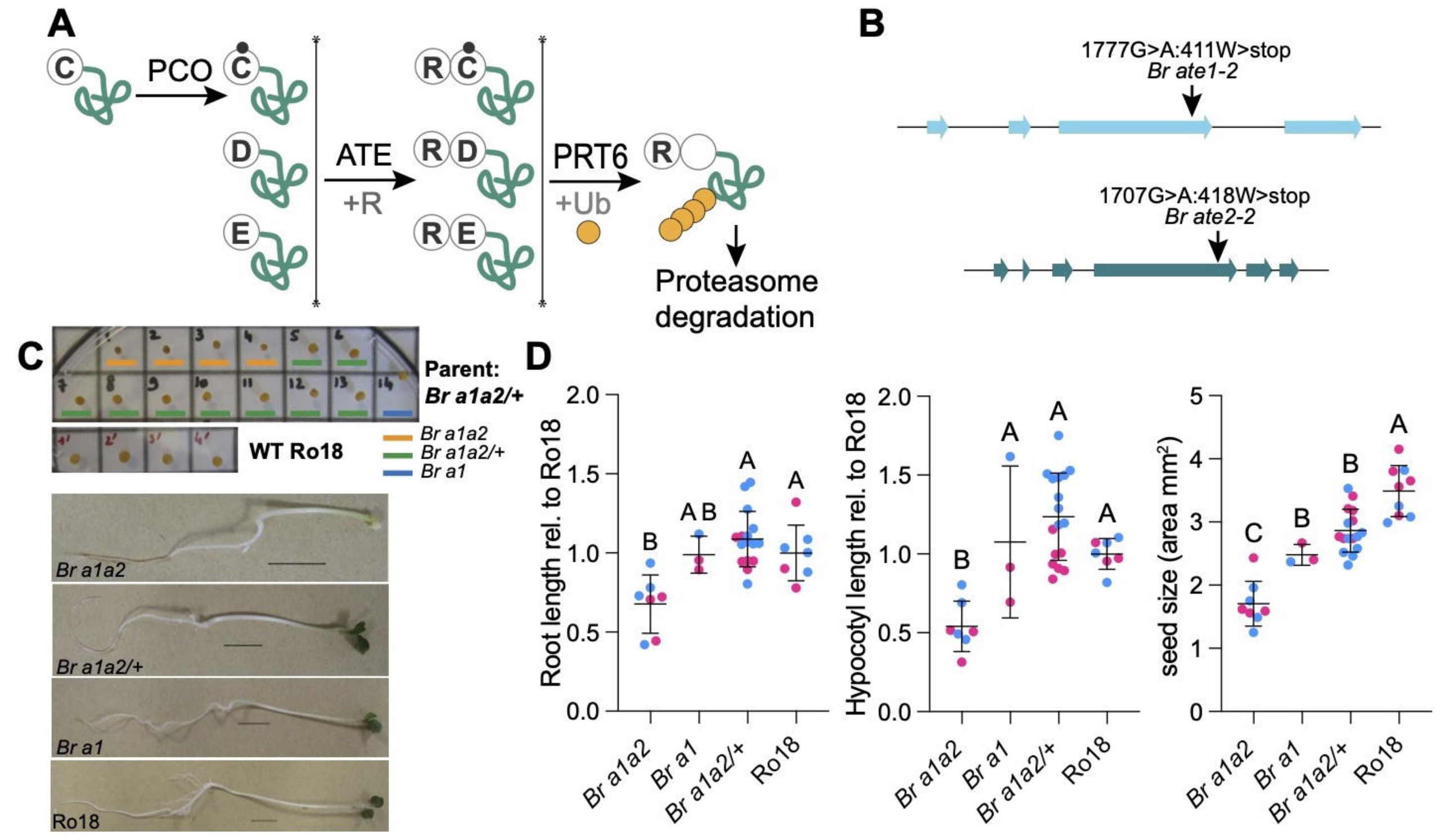
A
C
PCO
C
D
E
ATE
+R
R C
R D
R E
PRT6
+Ub
R
Proteasome degradation
B
1777G>A:411W>stop
Br ate1-2
1707G>A:418W>stop
Br ate2-2
C
Parent:
Br a1a2/+
WT Ro18
Br a1a2
Br a1a2/+
Br a1
Br a1a2
Br a1a2/+
Br a1
Ro18
D
Root length rel. to Ro18
Hypocotyl length rel. to Ro18
seed size (area mm²)
Br a1a2
Br a1
Br a1a2/+
Ro18

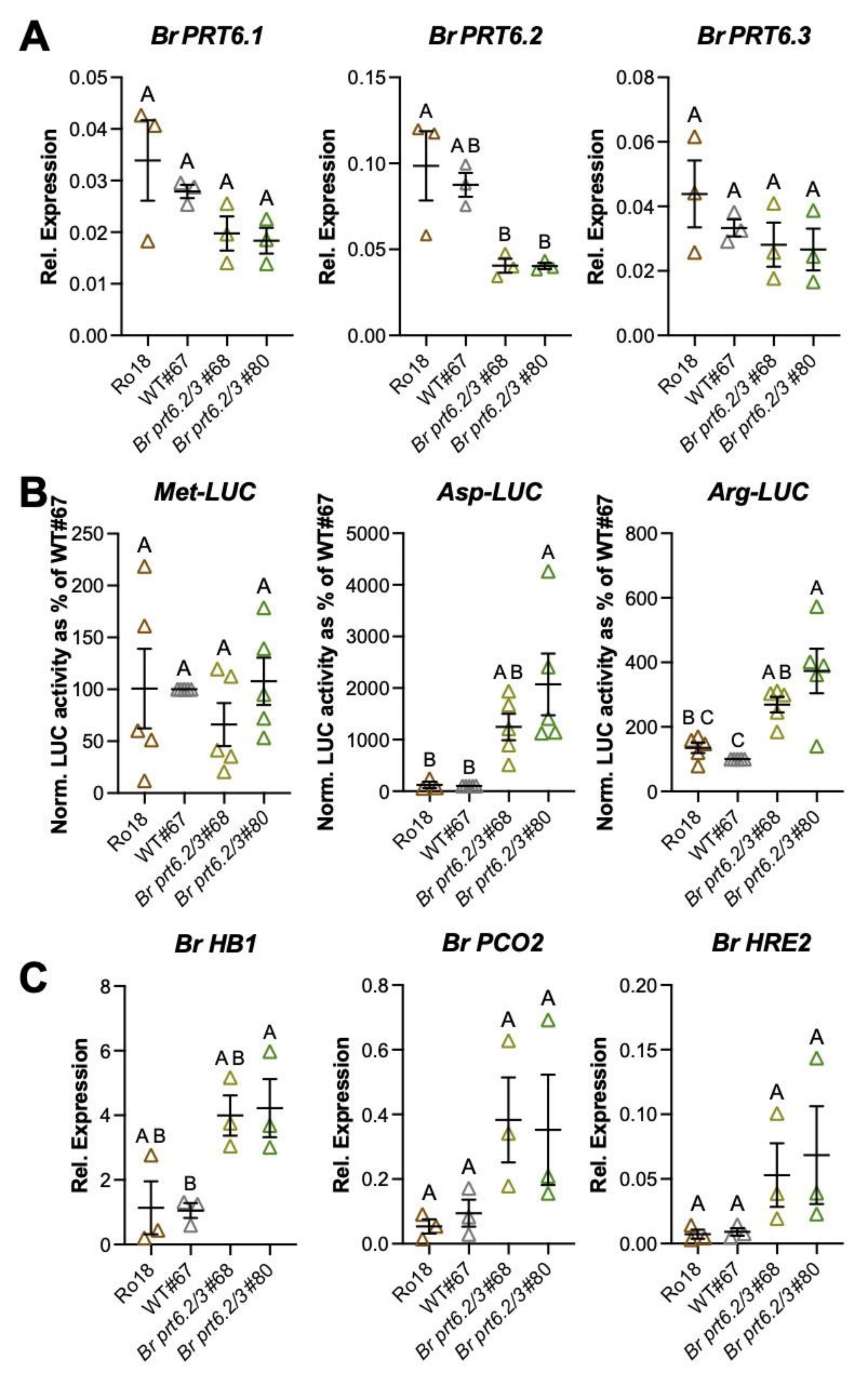
A
Br PRT6.1
Br PRT6.2
Br PRT6.3
Rel. Expression
Ro18
WT#67
Br prt6.2/3 #68
Br prt6.2/3 #80
B
Met-LUC
Asp-LUC
Arg-LUC
Norm. LUC activity as % of WT#67
Br prt6.2/3#68
Br prt6.2/3#80
C
Br HB1
Br PCO2
Br HRE2

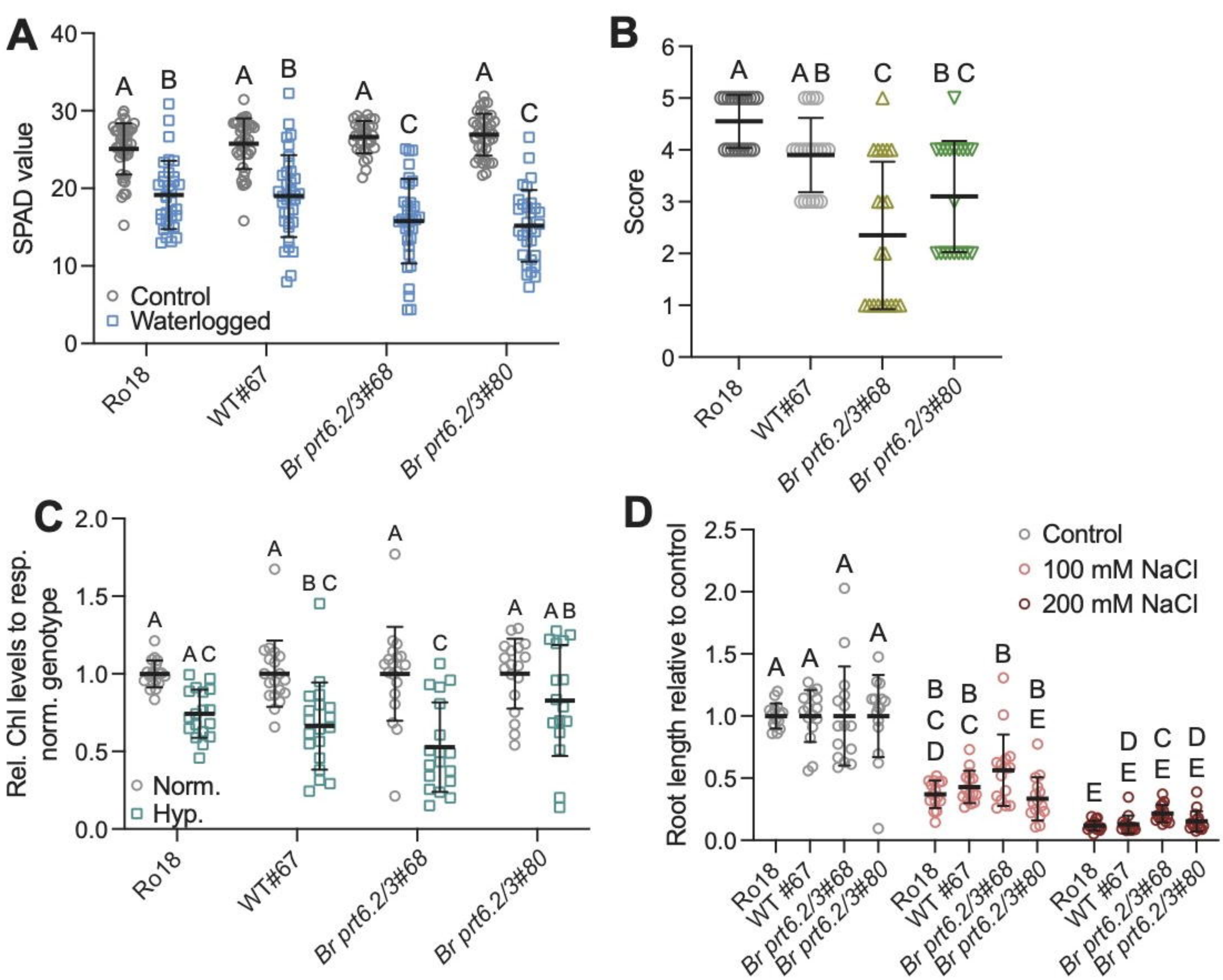
A
SPAD value
Control
Waterlogged
Ro18
WT#67
Br prt6.2/3#68
Br prt6.2/3#80
B
Score
C
Rel. Chl levels to resp. norm. genotype
Norm.
Hyp.
D
Root length relative to control
Control
100 mM NaCl
200 mM NaCl

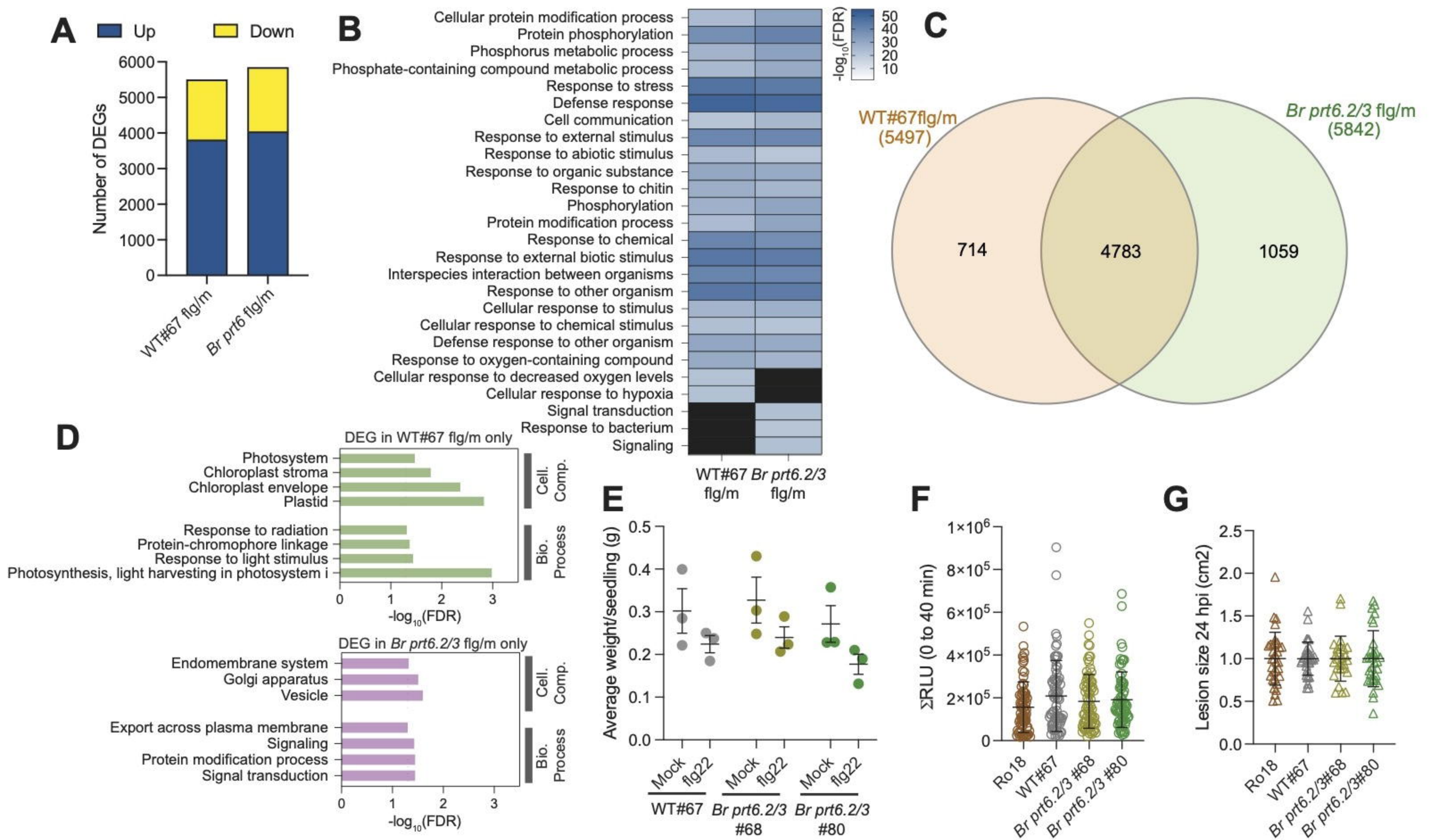
A
Up
Down
Number of DEGs
6000
5000
4000
3000
2000
1000
0
WT#67 flg/m
Br prt6 flg/m
B
Cellular protein modification process
Protein phosphorylation
Phosphorus metabolic process
Phosphate-containing compound metabolic process
Response to stress
Defense response
Cell communication
Response to external stimulus
Response to abiotic stimulus
Response to organic substance
Response to chitin
Phosphorylation
Protein modification process
Response to chemical
Response to external biotic stimulus
Interspecies interaction between organisms
Response to other organism
Cellular response to stimulus
Cellular response to chemical stimulus
Defense response to other organism
Response to oxygen-containing compound
Cellular response to decreased oxygen levels
Cellular response to hypoxia
Signal transduction
Response to bacterium
Signaling
WT#67 flg/m
Br prt6.2/3 flg/m
-log10(FDR)
50
40
30
20
10
C
WT#67flg/m (5497)
Br prt6.2/3 flg/m (5842)
714
4783
1059
D
DEG in WT#67 flg/m only
Photosystem
Chloroplast stroma
Chloroplast envelope
Plastid
Response to radiation
Protein-chromophore linkage
Response to light stimulus
Photosynthesis, light harvesting in photosystem i
Cell. Comp.
Bio. Process
-log10(FDR)
DEG in Br prt6.2/3 flg/m only
Endomembrane system
Golgi apparatus
Vesicle
Export across plasma membrane
Signaling
Protein modification process
Signal transduction
Cell. Comp.
Bio. Process
-log10(FDR)
E
Average weight/seedling (g)
Mock
flg22
WT#67
Br prt6.2/3 #68
Br prt6.2/3 #80
F
ΣRLU (0 to 40 min)
Ro18
WT#67
Br prt6.2/3 #68
Br prt6.2/3 #80
G
Lesion size 24 hpi (cm2)
Ro18
WT#67
Br prt6.2/3#68
Br prt6.2/3#80